Monte Carlo Simulations of Hypersonic Flows Past Blunt Bodies

W. Wetzel* and H. Oertel Jr.†
German Aerospace Research Establishment (DLR), Göttingen, Federal Republic of Germany

This paper reports on the steps taken to develop a gas-kinetic simulation of hypersonic flows past the nose region of re-entry vehicles. For the validation of both the direct simulation Monte Carlo (DSMC) and the molecular dynamics (MD) methods, the Oseen vortex decay problem was chosen to emphasize the conservation of angular momentum. Furthermore, an analytical solution of the Navier-Stokes equation exists for this problem. The results obtained with both methods correlate well with the analytical solution. The angular momentum is conserved exactly in the MD method; however, in the DSMC method, the cell sizes must be sufficiently small to conserve approximately the angular momentum because of the statistical assumptions. Both, the two- and three-dimensional DSMC-codes have been verified for the hypersonic flow past a circular cylinder and a sphere, respectively. The shock stand-off distance and the pressure distribution along the body surface were compared with experimental results. In both cases, the agreement is very good. As an application to more realistic configurations, the gaskinetic flow past the nose of a typical spacecraft is discussed for different Knudsen numbers.

Nomenclature

c = velocity vector, $\sqrt{u^2+v^2+w^2}$
c_{mp} = most probable thermal speed
c_p = pressure coefficient
$c_p(0)$ = pressure coefficient in stagnation point
Kn = Knudsen number
L = geometric property in Oseen-vortex
M = Mach number
R = radius cylinder
Δr = radial extent of cells
T = thermodynamic temperature
T_{int} = internal temperature
T_{ov} = overall kinetic temperature
T_{rot} = rotational kinetic temperature
T_{tr} = translational kinetic temperature
T_{vib} = vibrational kinetic temperature
η = ratio of specific heats
θ = angle range at cylinder
$\bar{\lambda}$ = mean free path
ρ = density

Subscripts

w = wall values
∞ = freestream values

Introduction

BECAUSE of the planning or development of new spacecrafts such as Hermes,[1] Hotol,[2] Sänger,[3] and future hypersonic airplanes,[4] there is renewed interest in understanding hypersonic flow. It is known that the development of the U.S. Space Shuttle relied heavily on experimental data obtained in wind tunnels and other experimental facilities. The experiences gained in free flight compared with the experimental and theoretical design are described in the literature.[5] These experiences show that quite a few flow phenomena lack basic understanding and require further studies. In contrast to the past design of the Space Shuttle, the Hermes vehicle is planned to be designed with the help of advanced numerical methods in order to reduce the expensive and time-consuming experimental investigations, especially in the rarefied flow regime of the re-entry trajectory.

The focus of the present study is the low-density region in the upper atmosphere, where numerical gaskinetic procedures are available to simulate hypersonic flows. High-speed flows under low density conditions deviate from a perfect gas behavior because of the excitation of rotation, vibration, and dissociation. At high altitudes, and therefore low density, the molecular collision rate is low and the energy exchange occurs under nonequilibrium conditions. For the simulation of such complicated flow phenomena, models and assumptions that must be checked separately are necessary.

Therefore, in this paper, the numerical gaskinetic codes are first applied to perfect gas and simple configurations. A subsequent application treats the flowfield simulation past a typical spacecraft nose under re-entry conditions. The simulation of gas viscosity and the excitation of internal modes have been approximated with gaskinetic models that are often used in an engineering context.[6]

Gaskinetic Procedures

In the transitional flow regime between continuum and free molecular flow, two gaskinetic simulation procedures, the molecular dynamics (MD)[7] simulation procedure and the direct simulation Monte Carlo (DSMC)[8] method, have been investigated[9] and applied.[10]

In the MD simulation procedure, the calculation starts with randomly positioning a given number of particles within the chosen control volume. The initial velocities of the particles are related to the physical problem; they can, for example, have a Maxwell distribution superimposed by a given macroscopic velocity. After the definition of the initial conditions, the particles move with their individual velocities. The change of the motion depends only on the chosen particle potential and the conditions at the boundaries of the computational domain. For the hard sphere potential, which has been assumed for all present MD results, there is no interaction between particles unless they collide with each other. Therefore, the time step must not be chosen larger than the time span between two subsequent collisions. Thus, in principle, for the estimation of the smallest time step, all possible collisions need to be checked. Then all molecules are moved according to this smallest time step, and just the single collision is then considered

Presented at the 16th International Symposium on Rarified Gas Dynamics, Pasadena, CA, July 10–16, 1988; received Nov. 2, 1988; revision received July 31, 1989.

*Dipl.-Ing., Institute for Theoretical Fluid Mechanics.
†Professor, Institute for Theoretical Fluid Mechanics; currently, Institute for Fluid Mechanics, Technical University of Braunschweig, Federal Republic of Germany.

based on the governing equations for fully elastic collisions.

Macroscopic quantities can be calculated at any time by sampling the properties of the particles. The advantage of this procedure is that no grid is required for the calculation, and it can therefore be applied to complex geometries. Although modifications to the MD method will speed up the computations considerably, it remains a very time-consuming method.

The DSMC method is similar to the MD procedure in that the paths of the model particles are determined, and the macroscopic quantities as obtained by sampling the microscopic quantities. The main difference between the methods exists in the treatment of the collisions where statistical assumptions are employed in the DSMC method. Because this results in less computational effort, the DSMC method is preferred. A detailed description of the DSMC method is given, for example, by Bird.[8]

Diatomic Simulation Models

The gas viscosity in the DSMC calculations was simulated by using the variable hard sphere (VHS) collision model of Bird.[6] In this model the temperature dependency of the viscosity is considered by a variable cross section that is inversely proportional to the relative collision energy between the colliding particles.

The internal energies of molecules have been considered with the phenomenological model introduced by Borgnakke and Larsen.[11] The essential feature of this model is that a part of the collisions is treated as completely inelastic. The probability for inelastic collisions, where energy transfer between translational and rotational energies may occur, is directly related to the rotational relaxation time. For the temperature range in our calculations, the rotational energy is always fully excited. At higher temperatures the vibrational degrees of freedom become excited.[12] To predict the degree of excitation at a particular temperature, the harmonic oscillator model has been used. The knowledge of the vibrational degrees of freedom enables the consideration of the translational-rotational and vibrational energy exchange in a modified version[13] of the Borgnakke-Larsen model. The proportion of such inelastic collisions is adjusted to the vibrational relaxation time.

Validation of the Gaskinetic Procedures

For the validation of the DSMC method and the MD procedure, the problem chosen was the decay of Oseen's vortex. This flow allows one to check the sensitivity of the DSMC method with respect to the conservation of angular momentum. The advantage of this test case is that there is an analytical solution of the Navier-Stokes equations, see for example Schlichting,[14] to compare within the transitional regime.

The control volume for the simulation of the vortex decay is sketched in Fig. 1. The characteristic length scale L of the problem is chosen to be the distance between the vortex center and initial location of the maximum of the velocity. At the boundary of the control volume, the model particles are reflected specularly, even though it is physically incorrect.

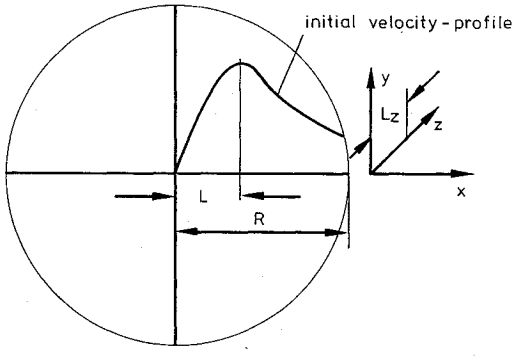

Fig. 1 Sketch of the simulation domain.

This way, however, the total amount of angular momentum within the control volume must remain constant. Thus, the conservation properties of the considered method can be checked directly. Knowing that the boundary condition is critical, care is taken that the influence of that condition does not penetrate too far in the direction of the vortex center. The extension of the disturbance can be limited by choosing the simulation time approximately, based on the fact that weak disturbances spread out with speed of sound. The interaction between the particles is considered with the hard sphere collision model.

In the case of the DSMC method the circular computational domain has been divided into cells as shown in Fig. 2. All cells have the same volume, and the radial extent of each cell is 0.8 mean free paths. Owing to the incompressible problem, the mean free path is almost the same in the whole flowfield and does not change strongly. The total number of particles is roughly 80,000.

Figure 3 shows for $Kn = 0.1$ a comparison of results for the MD and the DSMC method with the analytical solution in terms of velocity distribution. The velocity c is related to the most probably thermal speed c_{mp}. In the case of the MD method, 10,000 particles are employed for the simulation. The ratio between mean particle distance and particle diameter is 2.5. Eight independent runs have been made, and the corresponding results have been averaged. The agreement between the predicted and the analytical solution is good for both methods. As expected, some systematic disagreement is recognized near the boundary because of the chosen boundary condition.

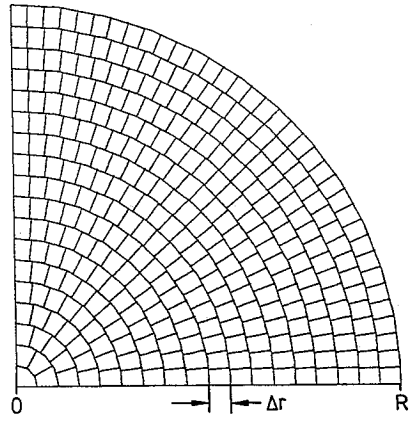

Fig. 2 Monte Carlo cell discretization.

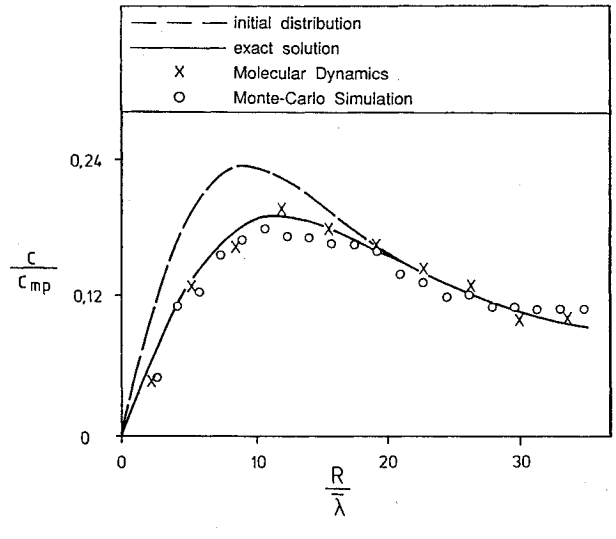

Fig. 3 Velocity distribution for $Kn = 0.1$.

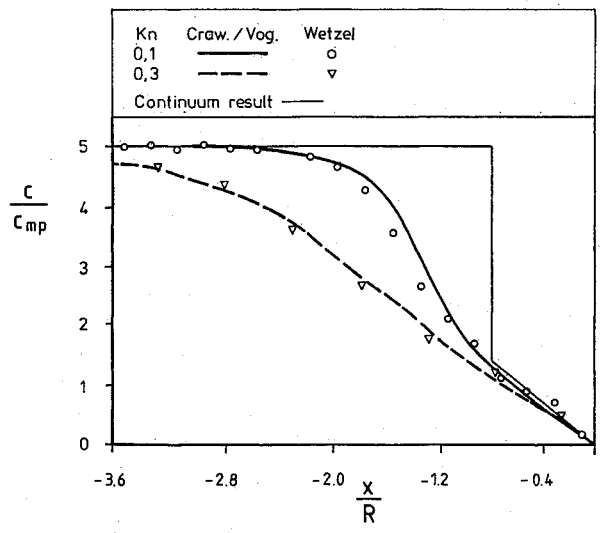

Fig. 4 Velocity profiles along the stagnation streamline ($M_\infty = 5.48$, adiabatic wall).

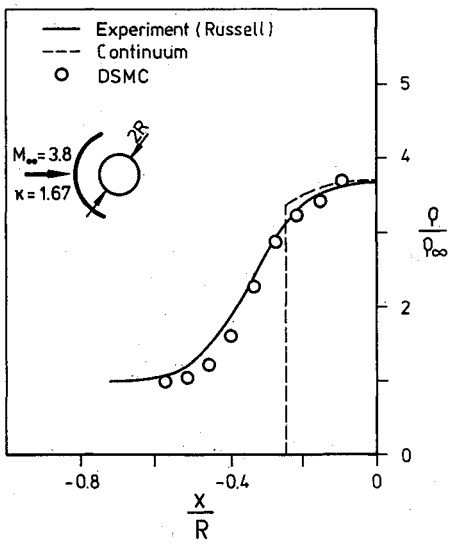

Fig. 6 Comparison of experimental and theoretical density profiles on the stagnation line of a sphere ($Kn = 0.06$, $M_\infty = 3.8$).

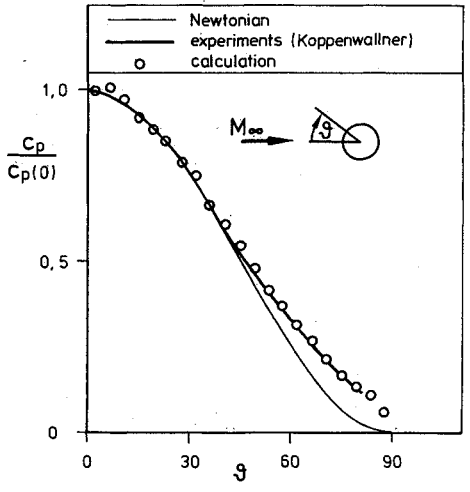

Fig. 5 Pressure distribution along the body surface ($M_\infty = 22.4$, $Kn = 0.1$; $T_w = 293$ K).

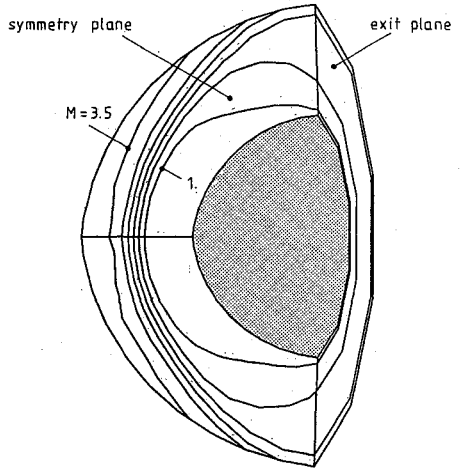

Fig. 7 Lines of constant Mach numbers in a perspective view.

After having investigated these two gaskinetic techniques, only the DSMC was used in the following because of its superior computational efficiency.

Comparison of Two-Dimensional and Three-Dimensional DMSC Results with Experiment

For the verification of the developed two-dimensional DSMC code, the adiabatic hypersonic flow past a circular cylinder is simulated, the fluid being argon. The calculations have been carried out with the VHS collision model for $Kn = 0.1$ and 0.3 and a freestream Mach number of 5.48. Diffuse reflection with complete thermal accommodation served as body surface boundary conditions. Particles are generated at the upstream boundary producing constant freestream conditions. The particles that leave the control volume will be neglected. The stationary state is achieved if the total number of particles does not change with time. After the stationary state is reached, time averages have been made to reduce the fluctuations in the simulation results. Similar investigations were carried out in 1974.[15] Therein, however, the inverse 12th-power-law potential was used in the collision model for Argon. Figure 4 shows the velocity distribution along the stagnation streamline in comparison with the simulation results of Crawford and Vogenitz.[15] The shock standoff distance is referenced to the radius R. An additional comparison is the continuum flow approximation, which has also been plotted in Fig. 4. One recognizes the shock wave building up in front of the body with reduced Kn with the shock thickness decreasing toward the continuum flow limit. The agreement between our DSMC simulation results and the literature results[15] is good.

As another test case, the DSMC method was applied to the hypersonic flow past an isothermal cylinder. The simulation of nitrogen molecules is carried out with the VHS collision model for $Kn = 0.1$, $M_\infty = 22.4$, and a wall temperature of 293 K. The internal energy exchange of the diatomic gas has been considered with the Borgnakke-Larsen[11] model. This test case was experimentally investigated by Koppenwallner.[16] In Fig. 5 the pressure distribution along the body surface is shown for the angle range of 0–90 deg. The comparison between measurement and simulation is very good. As expected, the Newtonian theory, which is also plotted in Fig. 5, deviates considerably from the experimental results for larger angles because the tangential momentum component dominates over the normal component for larger angles.

For the verification of the three-dimensional DSMC code, the supersonic flow past a sphere was simulated. The sphere serves as test body for the three-dimensional code as the circular cylinder for the two-dimensional code.

In Fig. 6, a comparison of the calculated results with electron beam measurements by Russell[17] is shown for the density

distribution along the stagnation streamline. The flowfield conditions are $M_\infty = 3.8$, $Kn = \bar{\lambda}/R = 0.06$. At the body surface, the adiabatic wall temperature was fixed. The predicted three-dimensional DSMC results are in a good agreement with the experimentally estimated density distribution ahead of the sphere.

Figure 7 shows the Mach-isolines in the calculated three-dimensional flowfield. The sonic line that separates the subsonic and supersonic region looks different in comparison to the continuum case. The calculated subsonic region extends around the front part of the sphere to the outflow boundary; emphasizing the low density effect on flow structure.

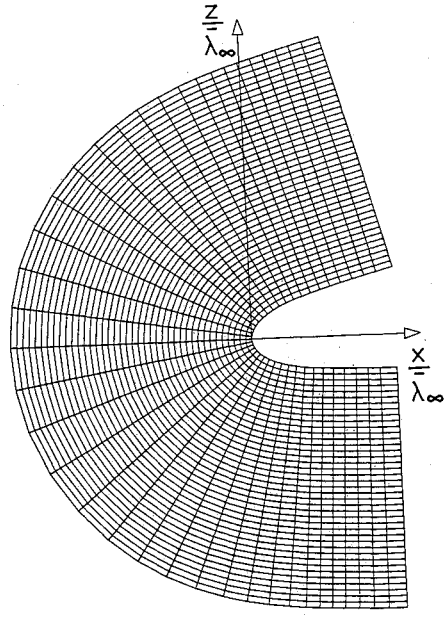

Fig. 8 Body-fitted cell discretization.

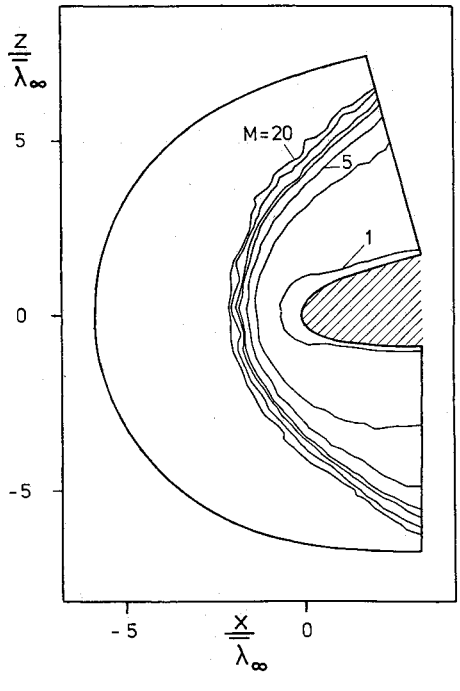

Fig. 9 Lines of constant Mach numbers ($Kn = 1.5$).

Application of the DSMC Method to a Typical Spacecraft Nose

In the following paragraphs, the two-dimensional flow simulation past the nose of a realistic spacecraft is discussed for different Knudsen numbers in the symmetry plane. The flow conditions are chosen from realistic re-entry parameters, and the boundary conditions are similar to the conditions given earlier. In Fig. 8 the body-fitted grid that we used for the flow simulation at $Kn = 1.5$ is shown. The cell sizes in the normal direction to the body are one mean free path of the undisturbed gas flow. This mean free path corresponds to an altitude of about 110 km, and the characteristic length is the aver-

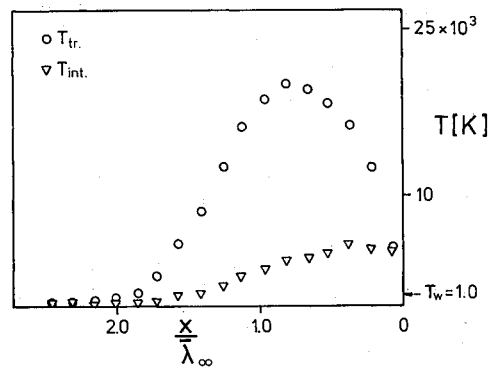

Fig. 10 Temperature distribution along the stagnation streamline ($Kn = 1.5$).

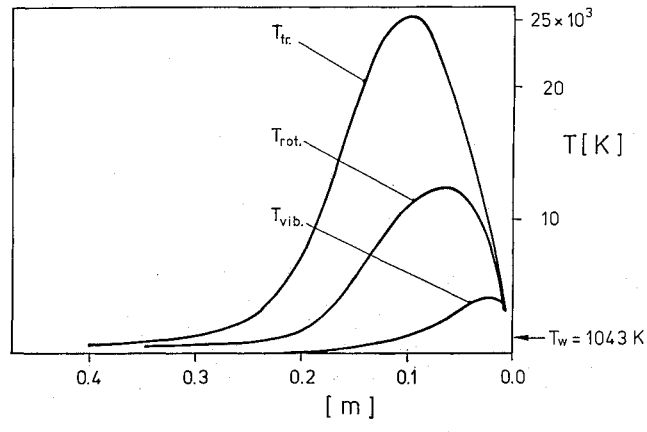

Fig. 11 Temperature components along the stagnation streamline. ($Kn = 0.08$).

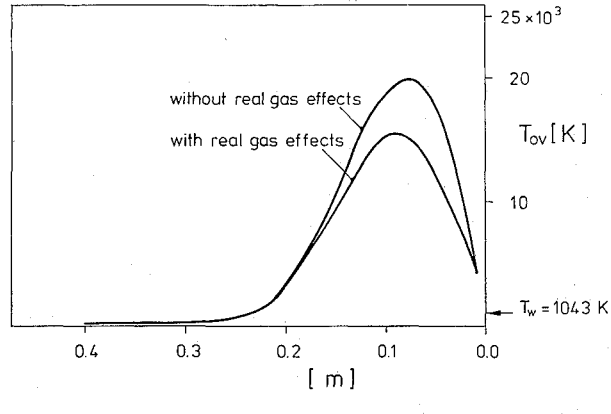

Fig. 12 Overall temperature distribution ($M_\infty = 24$, $Kn = 0.08$).

age nose radius in the symmetry plane. The grid chosen is only used to investigate the flow structure. It must be mentioned that especially for the prediction of heat flux into the body the resolution is not sufficient. In these initial calculations, the gas viscosity of nitrogen molecules has been simulated with the VHS collision model.

Figure 9 shows lines of constant Mach numbers in the symmetry plane of the flow past the typical spacecraft nose.

A shock layer in front of the nose is seen. The thickness is about two mean free paths, which corresponds to about 1.5 m. In Fig. 10 the temperature components along the stagnation streamline are plotted. The translational temperature increases across the shock wave to about 20,000 K. The large difference between translational temperature and internal temperature points out a strong nonequilibrium state of the flow near the stagnation point. This difference between the temperature components decreases at lower altitudes since the collision rate increases because of the higher density.

A further simulation was carried out at a Knudsen number of 0.08, corresponds to an altitude of about 95 km. Again the temperature components along the stagnation streamline are drawn (see Fig. 11). At this lower altitude, the vibrational degrees of freedom of the diatomic molecules are excited. Also, the difference between translational and rotational temperature becomes smaller because of the larger collision rate as mentioned earlier.

Figure 12 shows the overall temperature distribution along the stagnation line, with and without real gas effects. The differences are mainly due to the excitation of the vibrational modes. The overall temperature is defined as the weighted mean of the translational and internal temperature. It can be seen that, for the chosen parameters, the real gas effect causes approximately a 20% reduction in the maximum temperature.

Conclusion

This paper describes results of steps to develop a gas-kinetic simulation of hypersonic flowfields past blunt bodies. The validation of the MD procedure and the DSMC method in a vortex flow was carried out. It was shown that the DSMC is as good as the MD method even with respect to the conservation of angular momentum in vortical flows if the parameters of the method are chosen appropriately. For the simulation of hypersonic flowfields, the DSMC method is preferred to the MD method because of the larger computational efficiency.

For further validation, the two-dimensional and three-dimensional DSMC codes were applied to simulate the hypersonic/supersonic flow past a circular cylinder and a sphere. These simple bodies have been investigated experimentally in detail by many authors and are well suited for the verification of the numerical codes since real gas models are unnecessary for the low temperature ($T \lesssim 1500$ K) conditions. The comparison of the pressure distribution along the cylinder surface as well as the density distribution ahead of a sphere are in good agreement with the appropriate measurements. As an application to more realistic configurations, the hypersonic flow past the nose of a typical spacecraft was discussed for two different Knudsen numbers. The flow conditions in these calculations were similar to re-entry conditions. The simulation results show the strong nonequilibrium state across the shock wave in front of the body. At lower altitudes, nonequilibrium effects become smaller since the density and therefore the collision rate increases.

The next step will be the numerical investigation concerning real gas effects in fully three-dimensional hypersonic flows.

References

[1]Langereux, P., "Europe Aims for Space Independence," *Aerospace America,* Vol. 10, Special Rept., Feb. 1986.

[2]DeMeis, R., "HOTOL: The Other Aerospaceplane," *Aerospace America,* July 1986, pp. 10–12.

[3]Vogels, H. A., "Von der Mikrosystemtechnik zum Raumtransporter Sänger II," *Luft- und Raumfahrt,* Vol. 7, No. 4–86, Oct. 1986, pp. 99–108.

[4]Williams, R. M., "National Aero-Space Plane-Technology for America's Future," *Aerospace America,* Nov. 1986, pp. 18–22.

[5]Arrington, J. P., and Jones, J. J. (eds.), "Shuttle Performance: Lessons Learned," NASA CP-2283, 1983.

[6]Bird, G. A., "Monte-Carlo Simulation in an Engineering Context," *Rarefied Gas Dynamics,* edited by S. S. Fisher, Vol. 74, Progress in Astronautics and Aeronautics, AIAA, New York, 1981, pp. 239–255.

[7]Meiburg, E., "Comparison of the Molecular Dynamics Method and the Direct Simulation Monte Carlo Technique for Flows around Simple Geometries," *Physics of Fluids,* Vol. 29, Oct. 1986, pp. 3107–3113.

[8]Bird, G. A., *Molecular Gas Dynamics,* Clarendon, Oxford, UK, 1976.

[9]Wetzel, W., and Oertel, H., "Gas-Kinetical Simulation of Vortical Flows," *Acta Mechanica,* Vol. 70, 1987, pp. 127–143.

[10]Riedelbauch, S., Wetzel, W., Kordulla, W., and Oertel, H., Jr., "On the Numerical Simulation of Three-Dimensional Hypersonic Flow," AGARD CP-428, 1987.

[11]Borgnakke, C., and Larsen, P. S., "Statistical Collision Model for Monte-Carlo-Simulation of Polyatomic Gas Mixtures," *Journal of Computational Physics,* Vol. 18, Aug. 1975, pp. 405–420.

[12]Vincenti, W. G., and Kruger, C. H., *Introduction to Physical Gas Dynamics,* Wiley, New York, 1965.

[13]Bird, G. A., "Direct Molecular Simulation of a Dissociating Diatomic Gas," *Journal of Computational Physics,* Vol. 25, Dec. 1977, pp. 353–365.

[14]Schlichting, H., "*Boundary-Layer Theory,*" McGraw Hill, New York, 1979.

[15]Crawford, D. R., and Vogenitz, F. W., "Monte-Carlo Calculations for the Shock Layer Structure on an Adiabatic Cylinder in Rarefied Supersonic Flow," *Rarefied Gas Dynamics,* Deutsche Forschungs- und Versuchsanstalt für Luft- und Raumfahrt Press, Porz-Wahn, FRG, 1974.

[16]Koppenwallner, G., "Experimentelle Untersuchung der Druckver-teilung und des Widerstands von querangeströmten Kreiszylindern bei hypersonischen Machzahlen im Bereich von Kontinuums- bis freier Molekularströmung," *Zeitschrift fuer Flugwissenschaften,* Vol. 17, 1969, pp. 321–332.

[17]Russell, D. A., "Density Disturbance ahead of a Sphere in Rarefied Supersonic Flow," *Physics of Fluids,* Vol. 11, Aug. 1968, pp. 1679–1685.